Surface effect on the buckling of piezoelectric nanofilms

2012 J. Phys. D: Appl. Phys. 45 285301

(http://iopscience.iop.org/0022-3727/45/28/285301)

IOP PUBLISHING JOURNAL OF PHYSICS D: APPLIED PHYSICS

J. Phys. D: Appl. Phys. **45** (2012) 285301 (8pp) doi:10.1088/0022-3727/45/28/285301

Surface effect on the buckling of piezoelectric nanofilms

Jin Zhang, Chengyuan Wang and Sondipon Adhikari

College of Engineering, Swansea University, Singleton Park, Swansea, Wales SA2 8PP, UK

E-mail: chengyuan.wang@swansea.ac.uk (C Wang)

Received 9 February 2012, in final form 8 May 2012
Published 22 June 2012
Online at stacks.iop.org/JPhysD/45/285301

Abstract

A sandwich-plate model is developed to account for the effect of surface layers on the buckling of piezoelectric nanofilms (PNFs) due to an electrical voltage. The physical mechanisms of the surface effects are investigated and the contributions to the resultant effect are evaluated for surface piezoelectricity, surface stress and surface elasticity. It is found that the surface effect originates primarily from the residual surface stresses and enhanced piezoelectric coefficient due to the surface piezoelectricity. Its influence on the critical buckling voltage of a PNF depends sensitively on the thickness, the length-to-thickness ratio and the nature of residual surface stress. In addition, the intrinsic buckling may occur for a thin PNF where the relatively strong residual surface compression is achieved.

(Some figures may appear in colour only in the online journal)

1. Introduction

Piezoelectric nanostructures (PNs) have been synthesized in various configurations [1, 2], e.g. nanowires, nanofilms and nanorings. These smart nanomaterials exhibit enhanced piezoelectric effect, excellent resilience and the unique coupling between piezoelectric and semiconducting properties [1–3]. The distinct features make PNs promising for a wide range of applications in nanotechnology, such as nanosensors/transducers, nanogenerators, nanoresonators, diodes and piezoelectric field-effect transistors. The piezoelectric responses of PNs have thus become a current topic of great interest in recent research [4–13], where continuum piezoelectric theory was efficiently used as a cost-effective technique.

It is well-known that miniaturization of materials into a nanoscale size will significantly increase the surface-to-volume ratio. It thus may substantially improve the effect of the surface layers. This presumption has already been confirmed for elastic nanomaterials where significant surface effect leads to size-dependent elastic properties [14, 15] and the vibration and buckling behaviour distinct from those of their bulk counterparts [16, 17]. Recently, the size-dependent piezoelectric properties were reported for PNs in experiments [18] and simulations [19–21]. This infers that in addition to the surface stresses and surface elasticity, the surface piezoelectricity could also play a role in controlling the structural responses of PNs. However, most early studies of PNs [4–8] were based on the classical piezoelectric theory without considering the surface layers. Progress was made in a recent work by Wang and Feng [9], where an elastic surface layer was introduced. The effect of piezoelectric surface layers was first examined by Huang and Yu [10] for the static deformation of a piezoelectric nano-annular. The idea was further extended by Yan and Jiang [11, 12] to the study of the bending, buckling and vibration of piezoelectric nanobeams. Very recently, based on the one-dimensional beam theory Li *et al* [13] examined the effect of piezoelectric surface on the wrinkling of piezoelectric nanofilms (PNFs). Nevertheless PNFs as two-dimensional (2D) piezoelectric nanomaterials have not yet been studied so far due to lack of a reliable 2D model for PNFs. In particular, the physical mechanisms of the surface effect and the role of the surface stress, surface elasticity and surface piezoelectricity have not been discussed in detail.

To address these fundamental issues, this work aims to study the surface effect on the structural responses of 2D PNFs. In particular, the buckling induced by an electrical voltage is considered as it forms one of the major concerns for piezoelectric thin structures such as PNFs. A sandwich-plate model is first developed for the 2D piezoelectric nanomaterials by incorporating the surface effect and piezoelectric effect into

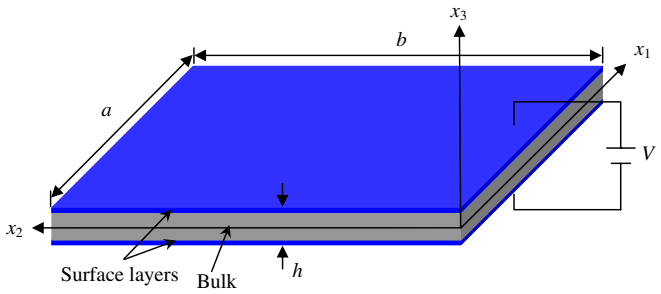

Figure 1. Illustration of a PNF as a composite plate comprising a core layer sandwiched by two surface layers. An electric voltage is applied in the thickness direction.

the classical plate theory. The resultant surface effects and its dependence on the geometric size of PNFs are studied in detail. The results are explained in terms of the contributions from the surface piezoelectricity, surface elasticity and surface residual stress. In addition, the shearing effect on the PNF buckling is also investigated by comparing different plate theories.

2. Sandwich-plate model

An isotropic rectangular PNF with width a, length b and constant thickness h is illustrated in figure 1. As seen from the illustration Cartesian coordinate system x_α ($\alpha = 1, 2, 3$) is used for the PNF, where the x_1x_2 plane coincides with its undeformed midplane and x_3 is in the direction of its thickness. The usual summation convention for repeated indices will be adopted with Greek indices ranging from 1 to 3 and Latin ones taking the values of 1 and 2. A comma represents differentiation with respect to the superscript index.

To account for the effect of the surface layers a PNF is considered as a composite plate comprising a core layer that is sandwiched between top and bottom thin surface layers (figure 1). The core plate has a constant thickness h (equal to the thickness of the PNF) and the same material properties as those of the bulk material. On the other hand, the two surface layers are treated as 2D plates with bending stiffness and in-plane extensional stiffness but negligible thickness. Residual stresses and the elastic, piezoelectric and dielectric properties different from those of the core layer are considered for the surface layers. In addition, a perfect bond is achieved between the core plate and the two surface layers, i.e. no slipping occurs between the two adjacent components, and the displacements are continuous in the sandwich plate. Here we first use Mindlin plate theory accounting for the effect of the shear deformation to derive the formulations. Following Mindlin's assumption the displacement field u_α at a point of the film (including the surface layers) can be represented by

$$u_i = u_i^0 - x_3\varphi_i, \qquad u_3 = u_3^0 \equiv w(x_i, t) \tag{1}$$

where u_α^0 is the displacement components of the midplane along the x_α direction, and φ_i is the rotation angle of a normal line due to plate bending with respect to x_i coordinates. In particular, φ_i can be approximated by $\varphi_i = w_{,i}$ for a Kirchhoff plate. Accordingly, the strains at an arbitrary point of PNFs can be written as

$$\varepsilon_{ij} = (u_{i,j} + u_{j,i})/2 = \gamma_{ij} - x_3(\varphi_{i,j} + \varphi_{j,i})/2, \tag{2}$$

$$\varepsilon_{i3} = (u_{3,j} + u_{j,3})/2 = (w_{,i} - \varphi_i)/2 \tag{3}$$

where $\gamma_{ij} = (u_{i,j}^0 + u_{j,i}^0)/2$ are the midplane strains describing the membrane deformations. The electric field is assumed to exist only in the x_3 direction, and related to the electric potential ϕ by

$$E_3 = -\phi_{,3}. \tag{4}$$

For the core layer of PNFs the stresses σ_{ij} and the electric displacement D_3 can be written as

$$\sigma_{\alpha\beta} = c_{\alpha\beta\gamma\delta}\varepsilon_{\gamma\delta} - e_{\alpha\beta3}E_3 \tag{5}$$

$$D_3 = e_{\alpha\beta3}\varepsilon_{\alpha\beta} + k_{33}E_3 \tag{6}$$

where $c_{\alpha\beta\gamma\delta}$, $e_{\alpha\beta3}$ and k_{33} are, respectively, the elastic, piezoelectric and dielectric constants for the bulk material. It is understood that the thickness of the surface layers is usually orders of magnitude smaller than the thickness of nanomaterials [22]. They are thus considered as two-dimensional (2D) surfaces (without thickness) in this work as well as previous studies of piezoelectric nanomaterials [10–12]. For such 2D surfaces the constitutive relations read [10–12]

$$\sigma_{ij}^s = \sigma_{ij}^0 + c_{ijkl}^s\varepsilon_{kl} - e_{ij3}^sE_3 \tag{7}$$

where σ_{ij}^s are membrane forces per unit length (or surface stresses), σ_{ij}^0 are residual membrane forces per unit length (or residual surface stresses), c_{ijkl}^s are the in-plane stiffnesses and e_{ij3}^s are the piezoelectric constants relating electric field and the membrane forces. In the absence of free electric charges, the electrostatic equilibrium condition requires that

$$D_{3,3} = 0. \tag{8}$$

Combining equations (1), (2), (4) and (8), and the electrical boundary conditions $\phi(-h/2) = 0$ and $\phi(h/2) = V$, the electric potential distribution is determined as

$$\phi = -\frac{1}{2k_{33}}e_{ij3}\varphi_{i,j}\left(x_3^2 - \frac{h^2}{4}\right) + \frac{V}{h}x_3 + \frac{V}{2}. \tag{9}$$

Substituting equations (2), (3) and (9) into equations (5) and (7) yields the stresses in the core and surface layers

$$\sigma_{ij} = c_{ijkl}\gamma_{kl} - x_3\bar{c}_{ijkl}\varphi_{k,l} + e_{ij3}V/h \tag{10}$$

$$\sigma_{i3} = c_{i3j3}(w_{,j} - \varphi_j) \tag{11}$$

$$\sigma_{ij}^s = \sigma_{ij}^0 + c_{ijkl}^s\gamma_{kl} - x_3\bar{c}_{ijkl}^sw_{,kl} + e_{ij3}^sV/h \tag{12}$$

where $\bar{c}_{ijkl} = c_{ijkl} + e_{ij3}e_{kl3}/k_{33}$ and $\bar{c}_{ijkl}^s = c_{ijkl}^s + e_{ij3}e_{kl3}^s/k_{33}$. The stress resultant $N_{i\alpha}$ and stress moment M_{ij} can be calculated by

$$\begin{aligned} N_{ij} &= \int_{-h/2}^{h/2}\sigma_{ij}\,\mathrm{d}x_3 + (\sigma_{ij}^{s+} + \sigma_{ij}^{s-}) \\ &= K_{ijkl}\gamma_{kl} + e_{ij3}V + 2\left(\sigma_{ij}^0 + e_{ij3}^s\frac{V}{h}\right) \end{aligned} \tag{13}$$

$$N_{i3} = \kappa \int_{-h/2}^{h/2} \sigma_{i3}\, \mathrm{d}x_3 = A\kappa c_{i3j3}(w_{,j} - \varphi_j) \tag{14}$$

$$M_{ij} = \int_{-h/2}^{h/2} x_3\sigma_{ij}\, \mathrm{d}x_3 + \frac{h}{2}(\sigma_{ij}^{s+} - \sigma_{ij}^{s-}) = -D_{ijkl}\varphi_{k,l}. \tag{15}$$

Here $\sigma_{ij}^{s\pm} = \sigma_{ij}^{s}|_{x_3=\pm h/2}$ are the stresses on the top and bottom surface layers, κ is the shear correction factor which usually has the value 5/6 [23] and D_{ijkl} and K_{ijkl} are the equivalent bending stiffness and in-plane extensional stiffness of the PNF, which are defined by

$$D_{ijkl} = \left((c_{ijkl} + e_{ij3}e_{kl3}/k_{33})I + (c_{ijkl}^{s} + e_{ij3}e_{kl3}^{s}/k_{33})\frac{h^2}{2}\right) \tag{16}$$

$$K_{ijkl} = Ac_{ijkl} + 2c_{ijkl}^{s} \tag{17}$$

where $(A, I) = \int_{-h/2}^{h/2}(1, x_3^2)\, \mathrm{d}x_3 = (h, h^3/12)$. It is seen in equations (16) and (17) that both surface piezoelectricity and surface elasticity contribute to the bending stiffness of a PNF while only the surface elasticity affects its in-plane extensional stiffness. On the other hand, the residual surface stress has no effect on the structural stiffnesses of a PNF. It only acts as in-plane stresses in equation (13), where the equivalent in-plane stresses can also be found due to the surface piezoelectricity.

In Mindlin's plate model, the equilibrium equation of a PNF is given as [23]

$$M_{ij,j} - N_{i3} = 0 \tag{18}$$

$$N_{i3,i} + N_{ij}w_{,ij} = 0. \tag{19}$$

Eliminating N_{i3} we can get the following equilibrium equation for a Kirchhoff plate:

$$M_{ij,ij} + N_{ij}w_{,ij} = 0. \tag{20}$$

Substituting equations (13)–(15) into equations (18) and (19) yields the equilibrium equation of PNFs as Mindlin plates

$$D_{ijkl}\varphi_{k,jl} + A\kappa c_{i3j3}(w_{,j} - \varphi_j) = 0 \tag{21}$$

$$A\kappa c_{i3j3}(w_{,ij} - \varphi_{j,i}) + \left[K_{ijkl}\gamma_{kl} + e_{ij3}V + 2\left(\sigma_{ij}^{0} + e_{ij3}^{s}\frac{V}{h}\right)\right]w_{,ij} = 0. \tag{22}$$

Its counterpart for PNFs as Kirchhoff plates is given by

$$D_{ijkl}w_{,ijkl} - \left[K_{ijkl}\gamma_{kl} + e_{ij3}V + 2\left(\sigma_{ij}^{0} + e_{ij3}^{s}\frac{V}{h}\right)\right]w_{,ij} = 0. \tag{23}$$

To simplify our analysis, without losing generality, throughout the paper we consider PNFs with all boundaries simply supported. The solutions to equations (21) and (22) of such PNFs take the form

$$\varphi_1(x_1, x_2) = \Psi_{1mn}\cos\left(\frac{m\pi}{a}x_1\right)\sin\left(\frac{n\pi}{b}x_2\right) \tag{24}$$

$$\varphi_2(x_1, x_2) = \Psi_{2mn}\sin\left(\frac{m\pi}{a}x_1\right)\cos\left(\frac{n\pi}{b}x_2\right) \tag{25}$$

$$w(x_1, x_2) = W_{mn}\sin\left(\frac{m\pi}{a}x_1\right)\sin\left(\frac{n\pi}{b}x_2\right) \tag{26}$$

where Ψ_{1mn}, Ψ_{2mn} and W_{mn} are constants; and m and n are the half wave numbers. Substituting equations (24)–(26) into equations (21) and (22), and solving V from the resulting eigenvalue problem, we can obtain the buckling voltage V for a PNF as a function of (m, n). The lowest value of V gives the critical buckling voltage V_{cr} of a PNF and associated (m, n) describes the buckling mode. Similarly, after substituting equation (26) into equation (23) and solving V from the resulting equation we can get V_{cr} and corresponding (m, n) for PNFs as Kirchhoff plates.

In figure 1, when the condition $b > a \gg h$ is satisfied, a PNF becomes a beam-like structure where the transverse displacement w is a function of x_2 but independent of x_1. In this case it can be proved (not shown in this paper) that equation (23) will reduce to the governing equation for the vibration of a piezoelectric nanobeam given in [12].

3. Results and discussion

In this section the sandwich-plate model and the analysis methods developed in section 2 will be employed to conduct a quantitative study of the buckling behaviour of PNFs. PZT-5H (a lead zirconate titanate material) is selected as an example for piezoelectric materials. For the core layer of a PNF the bulk material properties are used, i.e. $c_{11} = c_{22} = 126\,\mathrm{GPa}$, $c_{12} = 55\,\mathrm{GPa}$, $c_{44} = 35.3\,\mathrm{GPa}$, $e_{31} = e_{32} = -6.5\,\mathrm{C\,m^{-2}}$ and $k_{33} = 1.3 \times 10^{-8}\,\mathrm{C\,V^{-1}\,m^{-1}}$ [24]. For the surface layers, the material properties can be obtained by atomistic calculations or experiments. However, the accurate values of surface piezoelectric and dielectric constants are not yet available due to lack of such work on piezoelectric nanomaterials. Thus the values estimated in [10] are used in this study as an approximation, i.e. $c_{11}^{s} = c_{22}^{s} = 7.56\,\mathrm{N\,m^{-1}}$ and $e_{31}^{s} = e_{32}^{s} = -3 \times 10^{-8}\,\mathrm{C\,m^{-1}}$. Using an approximate ratio between different surface elastic constants [25], we obtain $c_{12}^{s} = 5.23\,\mathrm{N\,m^{-1}}$ and $c_{44}^{s} = 1.26\,\mathrm{N\,m^{-1}}$. In addition, $\sigma_{12}^{0} = 0$ is assumed on the surface layers [26] and the effect of the small middle-plane strains on the elastic buckling is neglected by assuming $\gamma_{ij} = 0$.

3.1. Buckling behaviour of PNFs

Here let us first study the buckling behaviours of PNFs induced by an electrical voltage applied in their thickness direction. The residual surface stresses of PNFs are taken as $\sigma_{11}^{0} = \sigma_{22}^{0} = 1\,\mathrm{N\,m^{-1}}$. In figure 2 the critical electrical voltage V_{cr} is calculated against the aspect ratio a/h for the PNFs of a thickness h (*a*) 20 nm, (*b*) 200 nm and (*c*) 2 μm, respectively. The ratio a/b grows from 0.25 to 0.5 and to 1. To examine the effect of shear deformation, the results obtained based on Kirchhoff plate theory are also presented in figure 2 in comparison with those of Mindlin plate theory.

Figure 2(*a*) (for $h = 20\,\mathrm{nm}$) shows that, with a given value of a/b the critical electric voltage V_{cr} decreases when the aspect ratio a/h grows (i.e. a PNF becomes thinner). For a fixed ratio a/h it declines with decreasing ratio a/b

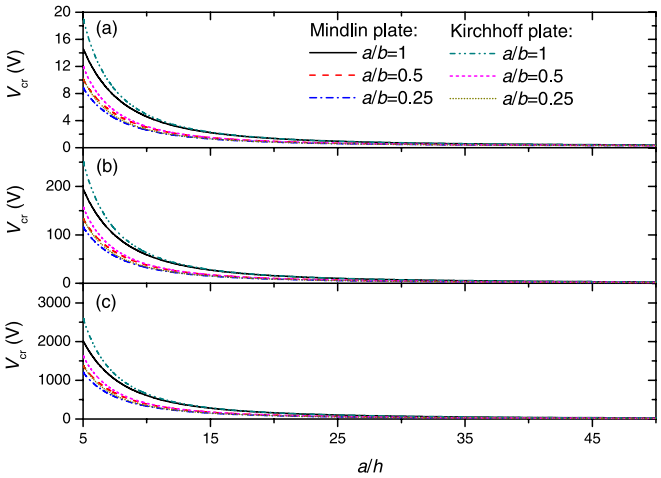

Figure 2. Critical buckling voltage V_{cr} versus the length-to-thickness ratio a/h obtained for PNFs whose thickness h is (a) 20 nm, (b) 200 nm and (c) 2 μm, respectively.

(i.e. a PNF becomes longer). When the thickness h increases to 200 nm and 2 μm, similar size-dependence of V_{cr} is found in figures 2(b) and (c) but the value of V_{cr} increases substantially in the process. For example, at h= 20 nm V_{cr} falls in the range (0.4 V, 19 V) when $a/b = 1$ and a/h varies between 5 and 50 (figure 2(a)). However, at $h = 200$ nm V_{cr} rises to 2.8 to 251 V in the same range of a/b and a/h (figure 2(b)). Obviously, this h-dependence of V_{cr} is a result of the enhanced bending stiffness of PNF*s* due to the increasing thickness h (equation (16)). Here it is worth mentioning that V_{cr} obtained in figure 2 always corresponds to the buckling mode $(m, n) = (1, 1)$ regardless of a/h, a/b and h considered.

In figure 2 the effect of shear deformation on the PNF buckling can be observed by comparing Mindlin plate theory considering shear deformation with Kirchhoff plate theory where the shearing effect is neglected. It is noted that the shear deformation reduces the critical buckling voltage V_{cr} significantly at a small ratio a/h. The effect then decreases with increasing a/h and finally becomes negligible at $a/h \geqslant 20$. According to this comparison result, the sandwich-plate model based on the Mindlin plate theory will be used in general cases to account for the effect of the shear deformation, while the model based on Kirchhoff theory will be used as an approximation in some special cases where $a/h \geqslant 20$ is satisfied. Here it is worth mentioning that when a/h is small the critical buckling voltage could be even higher than the critical voltage of the electrical breakdown. In this particular case the electric breakdown will occur before buckling. This phenomenon has not been discussed in detail in this study due to lack of reliable data in the literature. It, however, needs to be taken into consideration when PNFs are put into a practical use.

3.2. *Effect of surface layers*

Next we shall study the effect of the surface layers on the buckling of PNFs. To this end we have calculated the relative change in the critical buckling voltage $(V_{cr} - V_{cr}^0)/V_{cr}^0$ due to the surface effect, where V_{cr}^0 is the critical buckling voltage obtained without considering the surface effect, i.e. $\sigma_{ijkl}^0 = 0$, $c_{ijkl}^s = 0$ and $e_{ij3}^s = 0$. Previous studies [27, 28] showed that either residual surface tension or compression can be achieved for nanocrystals. Specifically, different surface stresses could alter the size-dependence of the surface effect on the buckling of PNFs. Thus, in this study we shall consider two cases: one is the PNFs made of PZT-5H where residual surface tension is found. The other is the PNFs made of a nanocrystal with residual surface compression. Here the objective is to capture the unique features of PNFs due to the surface compression. Thus the material properties of PZT-5H are still used in the second case.

The results obtained for PNFs with residual surface tension ($\sigma_{11}^0 = \sigma_{22}^0 = 1\,\mathrm{N\,m^{-1}}$) are plotted versus a/h in figure 3 with a/b equal to (a) 0.25, (b) 0.5 and (c) 1, respectively, and the thickness h varying from 20 nm, 200 nm to 2 μm. We can see from figure 3(a) that $(V_{cr} - V_{cr}^0)/V_{cr}^0$ curves associated with different thicknesses h intercept with the straight line $(V_{cr} - V_{cr}^0)/V_{cr}^0 = 0$ at exactly the same critical value of a/h, i.e. $(a/h)_{cr} = 24.1$ (see figure 3(a)). (1) At $a/h < (a/h)_{cr}$, i.e. PNFs are relatively thick, $(V_{cr} - V_{cr}^0)/V_{cr}^0$ is negative suggesting that the existence of the surface layers reduces the critical buckling voltage V_{cr}. Such a surface effect measured by the absolute value of $(V_{cr} - V_{cr}^0)/V_{cr}^0$ decreases when the aspect ratio a/h rises to approach $(a/h)_{cr}$, i.e. PNFs become thinner. (2) When a/h reaches the critical value $(a/h)_{cr}$, $(V_{cr} - V_{cr}^0)/V_{cr}^0$ goes to zero and the surface effect vanishes. (3) Further raising a/h to $a/h > (a/h)_{cr}$, i.e. PNFs are relatively thin, leads to positive $(V_{cr} - V_{cr}^0)/V_{cr}^0$ which increases with growing a/h. Thus the surface layers of the relatively thin PNFs can raise the critical buckling voltage. This effect becomes more pronounced for thinner PNFs with a greater aspect ratio a/h.

From these results it follows that the critical value $(a/h)_{cr}$ is independent of the thickness h and can classify PNFs into two groups which exhibit inverse surface effects that have opposing size-dependence on a/h. Further, it can also be seen from figure 3(a) that when h changes from 20 nm to 2 μm the absolute value of $(V_{cr} - V_{cr}^0)/V_{cr}^0$ decreases considerably and its dependence on a/h becomes very weak. Our numerical study shows that at $h > 720$ nm the absolute value of $(V_{cr} - V_{cr}^0)/V_{cr}^0$ is smaller than 5% throughout the range of a/h considered. In other words, for PNFs of $a/b = 0.25$, the surface effect is negligible when h exceeds this critical value $h_{cr} = 720$ nm. Similar behaviour of the surface effect is observed in figures 3(b) and (c) for the PNFs of ratio $a/b = 0.5$ and 1, respectively. But the critical aspect ratio $(a/h)_{cr}$ increases to 23.1 and 29.4 (figures 3(b) and (c)). In the meantime, our calculation shows that the critical thickness h_{cr} decreases to 580nm and 300nm, respectively.

The above size-dependence of $(a/h)_{cr}$ is obtained for constant surface stresses $\sigma_{11}^0 = \sigma_{22}^0 = 1\,\mathrm{N\,m^{-1}}$ and $a/b = 0.25, 0.5$ or 1. However, σ_{11}^0 and σ_{22}^0 may vary in the range 0.1to 1N m^{-1} [27, 28], which could alter the critical value $(a/h)_{cr}$. In addition, the ratio a/b usually changes continuously in the applications of PNFs. It is thus of interest to further study the dependence of $(a/h)_{cr}$ on the residual surface stresses and

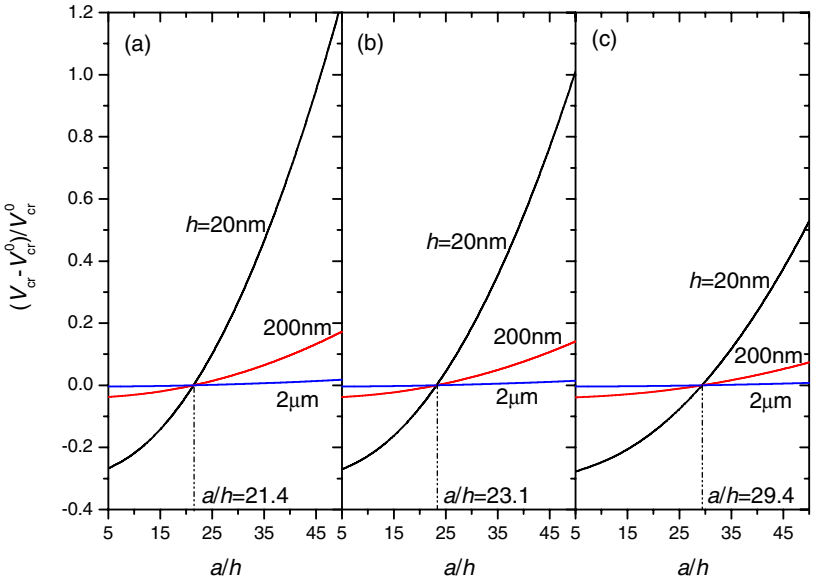

Figure 3. The relative change in the critical buckling voltage $((V_{cr} - V_{cr}^0)/V_{cr}^0)$ as a function of the length-to-thickness ratio a/h obtained for PNFs with positive residual surface stresses and (*a*) $a/b = 0.25$, (*b*) $a/b = 0.5$, (*c*) $a/b = 1$. Here V_{cr} is the critical electrical voltage obtained by considering surface effect and V_{cr}^0 is the one obtained without considering surface effect.

the ratio a/b. To simplify our analysis we consider relatively thin PNFs where $(a/h)_{cr} > 20$. In this case, Kirchhoff plate theory, i.e. equation (23), can be used. Equations (23) and (26) yield

$$\frac{V_{cr}}{V_{cr}^0} = \left[\frac{1}{1 + 2e_{31}^s/(e_{31}h)}\right] \cdot \left\{1 + \frac{6\pi^2[\bar{c}_{11}^s(1+\beta^4) + 2(\bar{c}_{12}^s + 2\bar{c}_{44}^s)\beta^2] + 24\alpha^2\sigma_{11}^0(1+\beta^2)}{\pi^2 h[\bar{c}_{11}(1+\beta^4) + 2(\bar{c}_{12} + 2\bar{c}_{44})\beta^2]}\right\} \tag{27}$$

where $\alpha = a/h$ and $\beta = a/b$. $(a/h)_{cr}(> 20)$ can be obtained based on equation (27) when $V_{cr}/V_{cr}^0 = 1$ is satisfied, i.e. the surface effect vanishes

$$\left(\frac{a}{h}\right)_{cr} = \{[\pi^2 e_{31}^s[\bar{c}_{11}(1+\beta^4) + 2(\bar{c}_{12} + 2\bar{c}_{44})\beta^2] - 3\pi^2 e_{31}[\bar{c}_{11}^s(1+\beta^4) + 2(\bar{c}_{12}^s + 2\bar{c}_{44}^s)\beta^2]] \times [12e_{31}\sigma_{11}^0(1+\beta^2)]^{-1}\}^{1/2}. \tag{28}$$

Based on equation (28) we show graphically in figure 4 the tendency of $(a/h)_{cr}$ to change with the residual surface (tensile) stresses and the ratio a/b. This figure provides guidance for evaluating the surface effect and its size-dependence on rectangular PNFs with residual surface tension.

Subsequently, we shall consider PNFs where negative residual surface stresses $\sigma_{11}^0 = \sigma_{22}^0 = -1\,\mathrm{N\,m^{-1}}$ are found. The relative change in the critical buckling voltage $(V_{cr} - V_{cr}^0)/V_{cr}^0$ is calculated in figure 5 against a/h for the PNFs whose thickness h is 20 nm, 200 nm and 2 μm, respectively, and ratio a/b equals (*a*) 0.25, (*b*) 0.5 and (*c*) 1. In this case, negative $(V_{cr} - V_{cr}^0)/V_{cr}^0$ is obtained throughout the range of the aspect ratio a/h considered. Its absolute value increases monotonically with rising a/h. These results indicate that with residual surface compression the surface layers always reduce the critical buckling voltage V_{cr} and the reduction of V_{cr} becomes greater for thinner PNFs of a greater aspect ratio a/h.

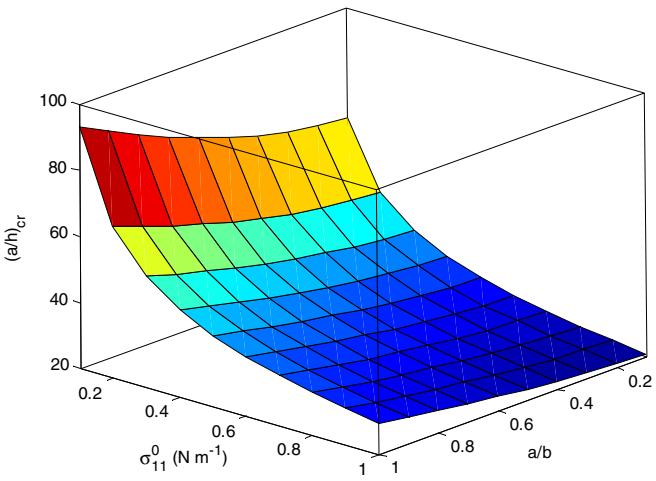

Figure 4. The dependence of the critical length-to-thickness ratio $(a/h)_{cr}$ on the residual surface stress and the aspect ratio a/b obtained for the PNFs with residual surface tension. Based on $(a/h)_{cr}$ the PNFs with residual surface tension can be categorized into two groups showing the inverse surface effects.

This behaviour is qualitatively different from that observed in figure 3 for the PNFs with residual surface tension. On the other hand, similar to what is shown in figure 3, the surface effect measured by the absolute value of $(V_{cr} - V_{cr}^0)/V_{cr}^0$ decreases substantially when h increases from 20 nm to 200 nm and to 2 μm. In particular, it is seen in figure 5 that when PNFs are sufficiently thin, e.g., $h = 20$ nm and $a/h = 34.5$ in figure 5(*a*), $(V_{cr} - V_{cr}^0)/V_{cr}^0$ is equal to negative one, i.e. $V_{cr} = 0$. This suggests that the intrinsic buckling would occur for thin PNFs due to the residual surface compression without any external mechanical or electrical loads. The experimental observation of this phenomenon has not yet been reported for PNFs in the literature. But the theory may provide a physical

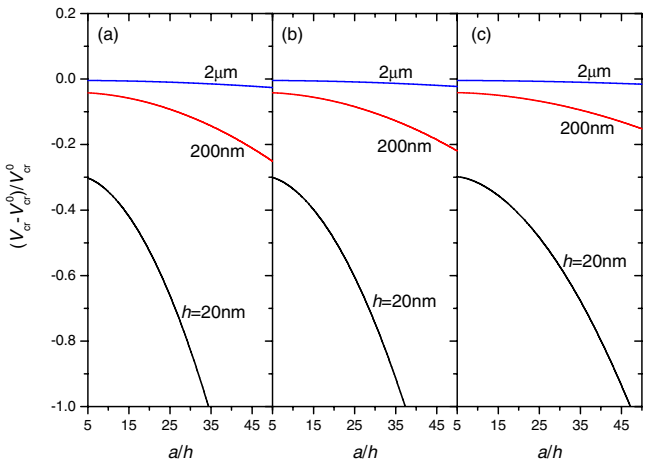

Figure 5. The relative change in the critical buckling voltage $((V_{cr}-V_{cr}^0)/V_{cr}^0)$ as a function of the length-to-thickness ratio a/h obtained for PNFs with negative residual surface stresses and (*a*) $a/b = 0.25$, (*b*) $a/b = 0.5$, (*c*) $a/b = 1$.

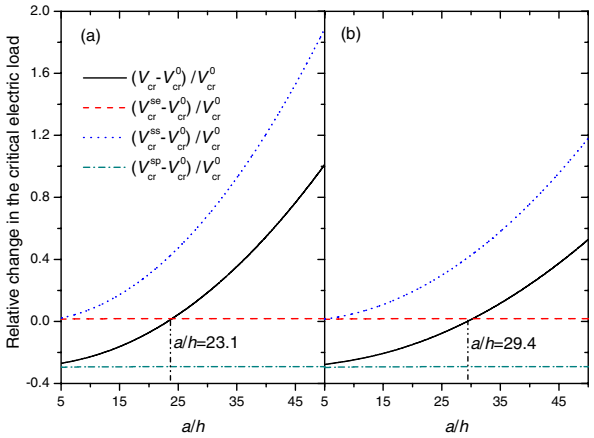

Figure 6. The a/h-dependence of the surface effect due to the surface elasticity, residual surface stress and surface piezoelectricity and all three factors. The results are obtained for PNFs with residual surface tension and (*a*) $a/b = 0.5$ and (*b*) $a/b = 1$. Here V_{cr}^{sp}, V_{cr}^{ss}, V_{cr}^{se}, V_{cr} and V_{cr}^0 are the critical buckling voltage calculated under following conditions, respectively, i.e. $\sigma_{ijkl}^0 = 0$, $c_{ijkl}^s = 0$, $e_{ij1}^s \neq 0$; $\sigma_{ijkl}^0 \neq 0$, $c_{ijkl}^s = 0$, $e_{ij1}^s = 0$; $\sigma_{ijkl}^0 = 0$, $c_{ijkl}^s \neq 0$, $e_{ij1}^s = 0$ and $\sigma_{ijkl}^0 \neq 0$, $c_{ijkl}^s \neq 0$, $e_{ij1}^s \neq 0$.

explanation for the intrinsic wrinkling observed for graphene sheets [29] where residual compressive stress is found [30] possibly due to the nonlocal interaction of carbon atoms in graphene [31].

3.3. Physical mechanisms of the surface effect

In principle, the surface effect is the resultant effect of the surface piezoelectricity, residual surface stress and surface elasticity. To understand the surface effects obtained in section 3.2 we shall first estimate the contributions of the three individual factors to the resultant effect and then study the physical mechanisms via which they exert influence on the buckling of PNFs.

First let us consider PNFs with residual surface tension $\sigma_{11}^0 = \sigma_{22}^0 = 1\,\mathrm{N\,m^{-1}}$. In figure 6 $(V_{cr}^{sp}-V_{cr}^0)/V_{cr}^0$, $(V_{cr}^{ss}-V_{cr}^0)/V_{cr}^0$, $(V_{cr}^{se}-V_{cr}^0)/V_{cr}^0$ and $(V_{cr}-V_{cr}^0)/V_{cr}^0$ are obtained for the PNFs under the conditions $\sigma_{ijkl}^0 = 0$, $c_{ijkl}^s = 0$, $e_{ij1}^s \neq 0$, $\sigma_{ijkl}^0 \neq 0$, $c_{ijkl}^s = 0$, $e_{ij1}^s = 0$, $\sigma_{ijkl}^0 = 0$, $c_{ijkl}^s \neq 0$, $e_{ij1}^s = 0$ and $\sigma_{ijkl}^0 \neq 0$, $c_{ijkl}^s \neq 0$, $e_{ij1}^s \neq 0$, respectively. Thus, these quantities measure the surface effect on the critical buckling voltage due to the surface piezoelectricity, residual surface stress, surface elasticity and all the three factors (i.e. the resultant surface effect). Here the film thickness is fixed at $h = 20\,\mathrm{nm}$, the aspect ratio a/h increases from 5 to 50 and the ratio a/b is equal to 0.5 (figure 6(*a*)) or 1 (figure 6(*b*)). First we see from figure 6 that the effect of the surface elasticity is negligible as compared with that of the surface piezoelectricity and residual surface stresses. This can be attributed to the fact that (1) the surface elasticity-induced increase in the bending stiffness D_{ijkl} (equation (16)) is too small to significantly change the critical buckling voltage. (2) Its contribution to the in-plane stresses (equation (13)) via the in-plane extensional stiffness K_{ijkl} (equation (17)) is completely neglected as γ_{ij} is assumed to be zero in this study. Thus in the following discussion we shall only consider the effect of the residual surface stresses and surface piezoelectricity.

In figure 6 the inverse effects on the critical buckling voltage are achieved for the residual surface tension and surface piezoelectricity, i.e. the former enhances the critical buckling voltage while the latter lowers it down. Moreover, strong size-dependence is observed for the effect of the surface tension in figure 6 where $(V_{cr}^{ss}-V_{cr}^0)/V_{cr}^0$ becomes greater when a/h grows and (or) a/b decreases. In sharp contrast, $(V_{cr}^{sp}-V_{cr}^0)/V_{cr}^0$ remains (almost) a constant (around -0.3) independent of a/h and a/b, i.e. the effect of the surface piezoelectricity exhibits negligible dependence on both a/h and a/b. Figure 6 shows that the competition between the inverse effects of the surface tension $((V_{cr}^{ss}-V_{cr}^0)/V_{cr}^0)$ and surface piezoelectricity $((V_{cr}^{sp}-V_{cr}^0)/V_{cr}^0)$ finally leads to the unique features of the resultant surface effect $((V_{cr}-V_{cr}^0)/V_{cr}^0)$ described in section 3.2 (also see figure 2). As noted in figure 6, at $a/h < (a/h)_{cr}$, the effect of the surface piezoelectricity is stronger, which yields negative $(V_{cr}-V_{cr}^0)/V_{cr}^0$. The effect of the surface tension, however, rises with growing a/h. When a/h approaches $(a/h)_{cr}$ it becomes strong enough to counteract the effect of the surface piezoelectricity and results in $(V_{cr}-V_{cr}^0)/V_{cr}^0 = 0$. Subsequently, at $a/h > (a/h)_{cr}$ the effect of the surface tension becomes greater and leads to positive $(V_{cr}-V_{cr}^0)/V_{cr}^0$. Similar calculation is also performed for the PNFs with residual surface compression $\sigma_{11}^0 = \sigma_{22}^0 = -1\,\mathrm{N\,m^{-1}}$. The results are presented in figure 7 where both the surface compression and the surface piezoelectricity decrease the critical buckling voltage. The size-dependences of $(V_{cr}^{ss}-V_{cr}^0)/V_{cr}^0$ and $(V_{cr}^{sp}-V_{cr}^0)/V_{cr}^0$ in figure 7 are found to be analogous to their counterparts in figure 6. As a result, $(V_{cr}-V_{cr}^0)/V_{cr}^0$ representing the resultant surface effect is always negative and its magnitude increases monotonically with the rising a/h (figures 5 and 7).

It is noticed in equation (13) that the significant effect of the residual surface stresses obtained in figures 2, 5, 6 and 7 originates solely from the in-plane stresses $2\sigma_{11}^0$ and $2\sigma_{22}^0$

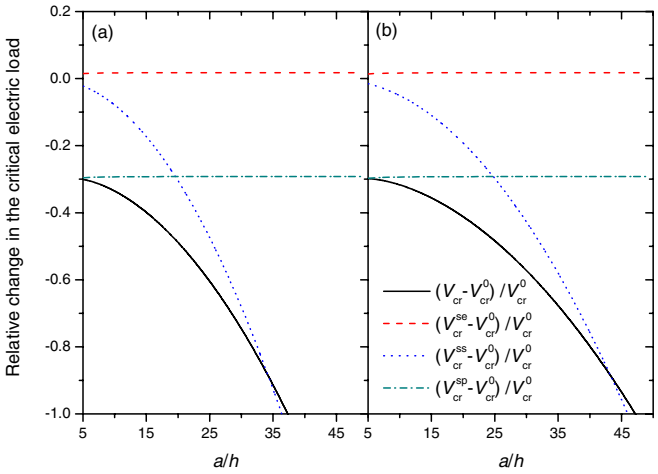

Figure 7. The a/h-dependence of the surface effect due to the surface elasticity, residual surface stress and surface piezoelectricity and all three factors. The results are obtained for PNFs with residual surface compression and (*a*) $a/b = 0.5$ and (*b*) $a/b = 1$.

due to the existence of the top and bottom surface layers. In other words the residual surface stresses change the critical buckling voltage by altering the effective structural rigidity of PNFs. Here the constant surface stresses are considered, whose influence on the buckling naturally increases when less rigid PNFs of greater a/h and (or) smaller a/b are concerned. This explains the size-dependence achieved in figures 6 and 7 for the effect of the constant residual surface stresses.

In addition, equations (13) and (16) show that piezoelectricity affects the structural responses of PNFs by (1) changing the equivalent bending stiffness via the electromechanical coupling, i.e. $(e_{ij3}/k_{33}) \cdot [e_{kl3} \cdot I + (h^2/2) \cdot e^s_{kl3}]$ (equation (16)) and (2) adding the equivalent in-plane stresses through the inverse piezoelectric effect, i.e. $[e_{ij3} + (2/h) \cdot e^s_{ij3}] \cdot V$ (equation (13)). In particular, the latter is actually the driving force that initiates the buckling of a PNF subject to an electrical voltage V. For the PNFs considered the change of the bending stiffness $(e_{ij3}/k_{33}) \cdot [e_{kl3} \cdot I + (h^2/2) \cdot e^s_{kl3}]$ is from around 3% to 6% of $c_{ijkl} \cdot 1$ when h varies between 20 and 200 nm. Here $c_{ijkl} \cdot 1$ is the bending stiffness of the elastic counterparts of the PNFs. Our numerical study shows that the effect on V_{cr} due to such a small change in the bending stiffness can be neglected in the buckling analysis. Thus the piezoelectricity (including the surface piezoelectricity) influences the structural responses of PNFs primarily through the equivalent in-plane stresses $[e_{ij3}+(2/h)\cdot e^s_{ij3}]\cdot V$ that are proportional to the applied voltage V and the equivalent piezoelectric coefficient $e_{ij3}+(2/h)\cdot e^s_{ij3}$. Based on these analyses we come to the conclusion that the surface piezoelectricity alters the critical buckling voltage as it generates extra in-plane stresses $((2/h) \cdot e^s_{ij3} \cdot V)$ on the PNFs by raising the equivalent piezoelectric coefficient from e_{ij3} of bulk material to $e_{ij3} + (2/h) \cdot e^s_{ij3}$ at the nanoscale.

Moreover, in equation (27), it can be shown that

$$\frac{6\pi^2[\bar{c}^s_{11}(1+\beta^4) + 2(\bar{c}^s_{12} + 2\bar{c}^s_{44})\beta^2] + 24\alpha^2\sigma^0_{11}(1+\beta^2)}{\pi^2 h[\bar{c}_{11}(1+\beta^4) + 2(\bar{c}_{12} + 2\bar{c}_{44})\beta^2]} \ll 1$$

is satisfied under the condition $\sigma^0_{11} = 0$ and $c^s_{ijkl} = 0$. Based on this inequality and equation (27) the relative change in the critical buckling voltage due to the surface piezoelectricity can be estimated as

$$\left|\frac{V_{cr} - V^0_{cr}}{V^0_{cr}}\right| \approx \frac{1}{(e_{31}/\Delta e) + 1} \qquad \text{and} \qquad \Delta e = \frac{2}{h} \cdot e^s_{31} \tag{29}$$

which is independent of $\alpha = a/h$ and $\beta = a/b$ but increases with rising Δe. Equation (27) and thus equation (29) hold true for thin PNFs of $\alpha = a/h \geqslant 20$ as they are based on Kirchhoff plate theory. However, our numerical results given by Mindlin plate theory show (figures 6 and 7) that equation (29) is still valid even at $5 \leqslant a/h \leqslant 20$. We therefore propose that equation (29) may be used to estimate the effect of the surface piezoelectricity in general cases and theoretically explain its negligible size-dependence on $\alpha = a/h$ and $\beta = a/b$.

4. Conclusions

A sandwich-plate model is developed for the voltage-induced buckling of piezoelectric nanofilms based on Mindlin's assumption and the theory of the surface effect. Using the model a detailed investigation is conducted regarding the surface effect on the critical buckling voltage and its dependence on the geometric size of the nanofilms. The major conclusions drawn in this study are summarized as follows:

(1) The physical origin of the surface effect is found to be the in-plane stresses produced by (a) the residual surface stresses $\sigma^0_{11} = \sigma^0_{22}$, and (b) the increase in the piezoelectric coefficient $(2/h) \cdot e^s_{ij3}$ due to the surface piezoelectricity. The surface elasticity, however, has negligible effect on the critical buckling voltage.

(2) The residual surface tension (or compression) increases (or decreases) the critical buckling voltage. The magnitude of the change rises with (a) the growing length-to-thickness ratio a/h and (b) the decreasing length-to-width ratio a/b. Differently the surface piezoelectricity here always reduces the critical buckling voltage. The reduction increases with $(2/h) \cdot e^s_{ij3}$ but is (almost) independent of a/h and a/b.

(3) The influence of the surface residual stresses and surface piezoelectricity yields the following resultant surface effect on the buckling of piezoelectric nanofilms. (a) For the nanofilms with residual surface tension, the surface layers decreases the critical buckling voltage when a/h is smaller than a certain critical value $(a/h)_{cr}$. Such an effect decreases with increasing a/h. Nevertheless, the surface effect and its dependence on a/h will be revised immediately once a/h exceeds $(a/h)_{cr}$. (b) For the nanoflims with residual surface compression, the surface layers always decrease the critical bucking voltage. This effect turns out to be stronger for a thinner nanofilms of a greater a/h. In particular, due to the surface compression, intrinsic buckling could occur for a thin nanofilm without any external loads.

Acknowledgments

JZ acknowledges the support from the China Scholarship Council (CSC). SA acknowledges the support from the Royal Society through the award of Wolfson Research Merit Award.

References

[1] Wang Z L 2007 *MRS Bull.* **32** 109
[2] Wang Z L 2009 *Mater. Sci. Eng.* R **64** 55
[3] Yang R, Qin Y, Li C, Zhu G and Wang Z L 2009 *Nano Lett.* **9** 1201
[4] Gao Y and Wang Z L 2007 *Nano Lett.* **7** 2499
[5] Tong H, Wang B L and Ou-Yang Z C 2008 *Thin Solid Film* **516** 2708
[6] Schubert M A, Senz S, Alexe M, Hesse D and Gosele U 2008 *Appl. Phys. Lett.* **92** 122904
[7] Shao Z Z, Wen L Y, Wu D M, Wang X F, Zhang X A and Chang S L 2010 *J. Phys. D: Appl. Phys.* **43** 245403
[8] Liang X and Shen S P 2012 *Smart Mater. Struct.* **21** 015001
[9] Wang G F and Feng X Q 2010 *Europhys. Lett.* **91** 56007
[10] Huang G Y and Yu S W 2006 *Phys. Status Solidi* b **243** R22
[11] Yan Z and Jiang L Y 2010 *J. Phys. D: Appl. Phys.* **44** 075404
[12] Yan Z and Jiang L Y 2011 *Nanotechnology* **22** 245703
[13] Li Y H, Fang B, Zhang J Z and Song J Z 2011 *J. Appl. Phys.* **110** 114303
[14] Lucas M, Mai W J, Yang R, Wang Z L and Riedo E 2007 *Nano. Lett.* **7** 1314
[15] Agrawal R, Peng B, Gdoutos E E and Espinosa H D 2008 *Nano Lett.* **8** 3668
[16] Wang G F and Feng X Q 2009 *J. Phys. D: Appl. Phys.* **42** 155411
[17] Wang G F and Feng X Q 2009 *Appl. Phys. Lett.* **94** 141913
[18] Zhao M H, Wang Z L and Mao S X 2004 *Nano. Lett.* **4** 587
[19] Xiang H J, Yang J, Hou J G and Zhu Q 2006 *Appl. Phys. Lett.* **89** 223111
[20] Li C, Guo W, Kong Y and Gao H 2007 *Appl. Phys. Lett.* **90** 033108
[21] Mitrushchenkov A, Linguerri R and Chambaud G 2009 *J. Phys. Chem.* C **113** 6883
[22] Gurtin M E, Markenscoff X and Thurston R N 1976 *Appl. Phys. Lett.* **29** 529
[23] Reddy J N 2007 *Theory and Analysis of Elastic Plates and Shells* (Boca Raton, FL: CRC Press)
[24] Srinivas S and Li J Y 2005 *Acta Mater.* **53** 4135
[25] Izumi S, Hara S, Kumagai T and Sakai S 2004 *Thin Solid Films* **467** 253
[26] Assadi A and Farshi B 2010 *J. Appl. Phys.* **108** 074312
[27] Miller R E and Shenoy V B 2000 *Nanotechnology* **11** 139
[28] He J and Lilley C M 2008 *Nano Lett.* **8** 1798–802
[29] Fasolino A, Los J H and Katsnelson M I 2007 *Nature Mater.* **6** 858
[30] Lee C, Wei X D, Kysar J W and Hone J 2008 *Science* **321** 385
[31] Wang C Y, Murmu T and Adhikari S 2011 *Appl. Phys. Lett.* **98** 153101